

Discovery and characterization of 2-acylaminoimidazole mPGES-1 inhibitors

Matthew Allen Schiffler, Stephen Antonysamy, Shobha N Bhattachar, Kristina M Campanale, Srinivasan Chandrasekhar, Bradley Condon, Prashant V Desai, Matthew J. Fisher, Christopher Groshong, Anita K Harvey, Michael J Hickey, Norman E Hughes, Scott A Jones, Euibong James Kim, Steven L. Kuklish, John G. Luz, Bryan H Norman, Richard E Rathmell, John R Rizzo, Thomas W Seng, Stefan J Thibodeaux, Timothy A Woods, Jeremy S York, and Xiao-Peng Yu

J. Med. Chem., **Just Accepted Manuscript** • DOI: 10.1021/acs.jmedchem.5b01249 • Publication Date (Web): 10 Dec 2015

Downloaded from <http://pubs.acs.org> on December 12, 2015

Just Accepted

“Just Accepted” manuscripts have been peer-reviewed and accepted for publication. They are posted online prior to technical editing, formatting for publication and author proofing. The American Chemical Society provides “Just Accepted” as a free service to the research community to expedite the dissemination of scientific material as soon as possible after acceptance. “Just Accepted” manuscripts appear in full in PDF format accompanied by an HTML abstract. “Just Accepted” manuscripts have been fully peer reviewed, but should not be considered the official version of record. They are accessible to all readers and citable by the Digital Object Identifier (DOI®). “Just Accepted” is an optional service offered to authors. Therefore, the “Just Accepted” Web site may not include all articles that will be published in the journal. After a manuscript is technically edited and formatted, it will be removed from the “Just Accepted” Web site and published as an ASAP article. Note that technical editing may introduce minor changes to the manuscript text and/or graphics which could affect content, and all legal disclaimers and ethical guidelines that apply to the journal pertain. ACS cannot be held responsible for errors or consequences arising from the use of information contained in these “Just Accepted” manuscripts.

Discovery and characterization of 2-acylaminoimidazole mPGES-1 inhibitors

Matthew A. Schiffler,^{a,*} Stephen Antonysamy,^b Shobha N. Bhattachar,^a Kristina M. Campanale,^a Srinivasan Chandrasekhar,^{a,†} Bradley Condon,^b Prashant V. Desai,^a Matthew J. Fisher,^a Christopher Groshong,^b Anita Harvey,^{a,†} Michael J. Hickey,^b Norman E. Hughes,^a Scott A. Jones,^a Euibong J. Kim,^{a,‡} Steven L. Kuklish,^a John G. Luz,^b Bryan H. Norman,^a Richard E. Rathmell,^c John R. Rizzo,^a Thomas W. Seng,^a Stefan J. Thibodeaux,^{a,§} Timothy A. Woods,^a Jeremy S. York,^a and Xiao-Peng Yu^a

^aLilly Research Laboratories, A Division of Eli Lilly and Company, Indianapolis, Indiana 46285, USA

^bEli Lilly Biotechnology Center, San Diego, CA 92121, USA

^cLilly Research Laboratories, A Division of Eli Lilly and Company, Windlesham, Surrey GU20 6PH, United Kingdom

KEYWORDS: mPGES-1, aminoimidazole, clinical candidate

ABSTRACT: As part of a program aimed at the discovery of anti-nociceptive therapy for inflammatory conditions, a screening hit was found to inhibit *m*PGES-1 with an IC₅₀ of 17.4 μM. Structural information was used to improve enzyme potency by over 1000-fold. Addition of an appropriate substituent alleviated time-dependent CYP3A4 inhibition. Further SAR studies led to **8**, which had desirable potency (IC₅₀ = 12 nM in an *ex vivo* human whole blood (HWB) assay) and ADME properties. Studies on the formulation of **8** identified **8**•H₃PO₄ as suitable for clinical development. Omission of a lipophilic portion of the compound led to **26**, a readily orally bioavailable inhibitor with potency in HWB comparable to celecoxib. Furthermore, **26** was selective for *m*PGES-1 inhibition *versus* other mechanisms in the prostanoid pathway. These factors led to the selection of **26** as a second clinical candidate.

INTRODUCTION

For millennia, it has been known that willow bark possesses analgesic properties.^{1,2} However, only in the 19th century was the active component, salicylic acid, identified,³ and only much later did related research reveal that reduction in systemic PGE₂ levels correlated with an analgesic effect.⁴⁻⁶ Therapies indirectly modulating PGE₂ through inhibition of COX enzymes include such well-known and widely-available drugs as aspirin,⁷ naproxen, and ibuprofen.⁸ These drugs non-selectively inhibit both COX-1, a constitutive enzyme; and COX-2, which is induced during the inflammatory response.⁹ In recent years, selective COX-2 inhibitors have entered the market as treatments for pain.^{10,11}

However, in addition to suppressing PGE₂ production, COX-2 inhibition disrupts the downstream balance of TXA₂ and PGI₂ (Figure 1), which is thought to lead to an increased risk of thrombotic events.¹² Such observations have, in fact, led to the withdrawal of COX-2 inhibitors such as rofecoxib and valdecoxib from the market.¹³ Therefore, inhibition of targets further downstream in the prostaglandin pathway might be desirable.¹⁴ One such approach would entail direct inhibition of a PGE₂ synthase.

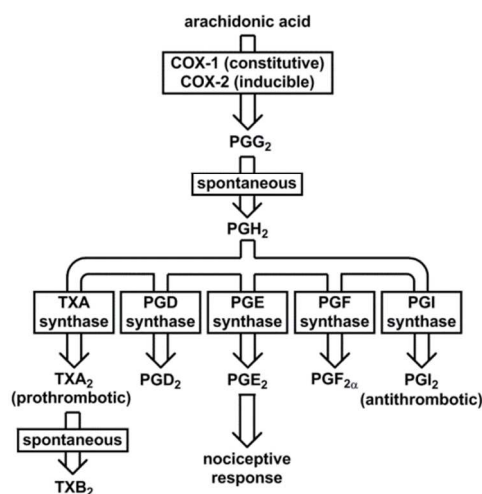


Figure 1. Prostaglandin synthesis pathway.

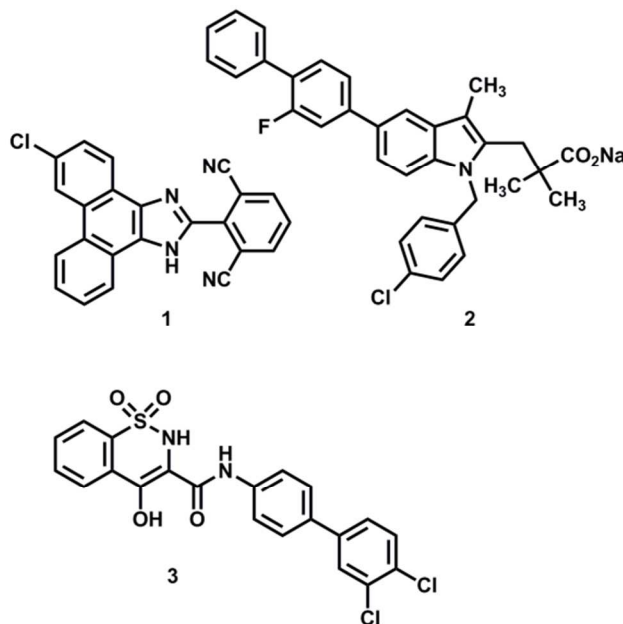
Microsomal prostaglandin E synthase-1 (*mPGES-1*) is a 17-kDa membrane-bound, glutathione-dependent isomerase which, like COX-2, is induced during the inflammatory response.¹⁵ It is one of three enzymes known to convert PGH₂ to PGE₂; the other two (*mPGES-2* and *cPGES*) are constitutively

expressed enzymes,¹⁶ and evidence has emerged that *m*PGES-2 does not in fact produce PGE₂ *in vivo*.¹⁷ Therefore, it has been hypothesized that selective inhibition of *m*PGES-1 could alleviate the nociception that accompanies inflammation while limiting the disruption of normal PGE₂ synthesis.¹⁸ Indeed, much effort has been made to discover *m*PGES-1 inhibitors.^{16–23} Chart 1 illustrates some examples of such compounds. Imidazophenanthrolines such as MF-63 (**1**),²⁰ aryl indoles such as **2**,²¹ and oxicams such as PF-9184 (**3**)²² have each been shown to inhibit *m*PGES-1. In addition, an *m*PGES-1 inhibitor known as GRC-27864 has entered clinical trials for inflammatory pain.²⁴

For the above reasons, we set out to identify an inhibitor of *m*PGES-1. We tested potency in a microsomal prep enzyme inhibition assay, and we measured PGE₂ and PGI₂ by EIA in hIL-1β-stimulated A549 cells to further evaluate potency and selectivity against other enzymes in the prostaglandin pathway.²⁵ It has been shown for COX-2 inhibitors that the IC₈₀ in an *ex vivo* LPS-stimulated human whole blood (HWB) assay (determined by measuring inhibition of PGE₂ response) correlates with efficacious *in vivo* therapeutic concentrations.²⁶ Therefore, we elected to evaluate our compounds by an analogous assay, using PGE₂ as a biomarker. Additionally in this assay, we measured TXB₂ and PGF_{2α} as selectivity readouts.²⁷

Celecoxib has been reported²⁸ to have a HWB IC₅₀ of 540 ± 70 nM.²⁹ In humans, a 200 mg oral dose of celecoxib results in a plasma drug concentration exceeding this IC₅₀ value for 8–12 hours.³⁰ Our aim was to find a selective *m*PGES-1 inhibitor amenable to a dosing regimen that would produce a similar or superior relationship of exposure to HWB potency.

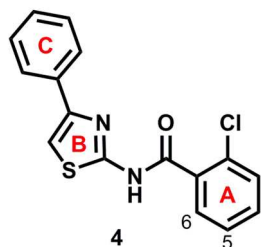
Chart 1. Examples of known *m*PGES-1 Inhibitors.



RESULTS AND DISCUSSION

In a screen of compounds from the Lilly collection, **4** (Chart 2) was identified in the enzyme assay as an *m*PGES-1 inhibitor ($IC_{50} = 17.4 \mu\text{M} \times/\div 1.25 (n = 2)$).³¹ The x-ray co-crystal structure of **4** with *m*PGES-1³² revealed a hydrogen bond between the benzamide nitrogen and His53, and showed that the C(5)-C(6) region of the A ring projected toward a cleft in the enzyme surface (Figure 2).

Chart 2. Initial screening hit.



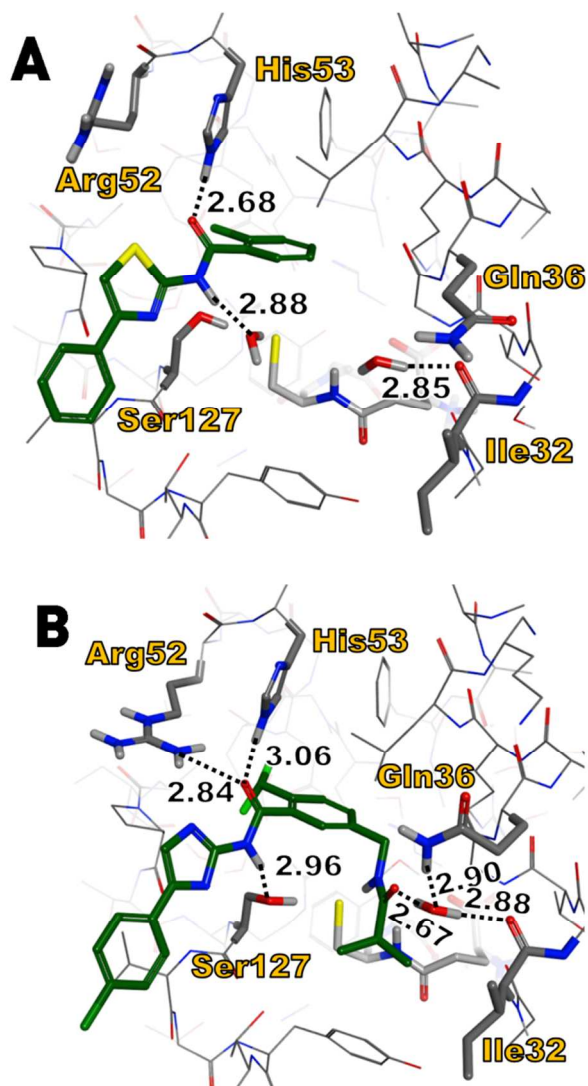
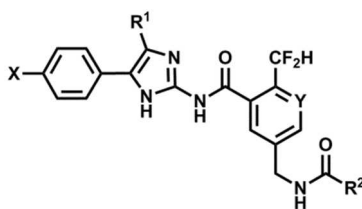


Figure 2. X-ray co-crystal structures of mPGES-1 with **4** (A) and **5** (B). Ligands, key side chains, and glutathione cofactors are highlighted with thick bonds. Some atoms omitted for clarity. H-bond distances given in Å.

Table 1. SAR of mPGES-1 Inhibitors **5–10** compared to reference compounds **1** and **2**.



comp	X	Y	R ¹	R ²	mPGES-1	A549	HWB	HWB	Microso-	Microso-	clog

d					IC ₅₀ ^a	PGE ₂ IC ₅₀ ^a	PGE ₂ IC ₅₀ ^a	PGE ₂ IC ₈₀ ^a	mal CYP3A4 inh. @ 10 μM (%)	mal CYP3A4 TDI @ 10 μM (%)	P ^c
1	n/a	n/a	n/a	n/a	5.3 nM ×/÷ 1.51 (239)	76 nM ×/÷ 2.16 (234)	676 nM ×/÷ 1.96 (61)	3.65 μM ×/÷ 2.23 (52)	32	NT	5.58
2	n/a	n/a	n/a	n/a	19.5 nM ×/÷ 1.84 (318)	1230 nM ×/÷ 1.21 (12)	NT	NT	46	NT	10.0
5	Cl	CH	H	<i>i</i> -Pr	<3 nM (2)	19 nM ×/÷ 1.59 (2)	338 nM ×/÷ 1.65 (6)	994 nM ×/÷ 1.57 (6)	44	75	4.38
6	Cl	N	H	<i>i</i> -Pr	<3 nM (3)	37 nM ×/÷ 1.04 (2)	29 nM ×/÷ 2.06 (5)	146 nM ×/÷ 2.46 (5)	22	72	3.32
7	Cl	N	CH ₃	<i>i</i> -Pr	<3 nM (5)	39 nM ×/÷ 1.43 (2)	91 nM ×/÷ 1.58 (5)	480 nM ×/÷ 2.35 (5)	0	27	3.45
8	CF ₃	N	CH ₃	<i>i</i> -Pr	0.9 nM ×/÷ 1.80 (10) ^b	12 nM ×/÷ 1.55 (4)	12 nM ×/÷ 1.94 (11)	69 nM ×/÷ 1.72 (11)	0	23	3.72
9	CF ₃	N	CH ₃	Et	10.3 nM	98 nM	374 nM	991 nM	0	15	3.18

					\times/\div 1.53	\times/\div 1.08	\times/\div 1.49	\times/\div 1.52			
					(5)	(2)	(3)	(3)			
10	CF ₃	N	CH ₃	CH ₃	74 nM \times/\div 1.17 (2)	720 nM (1)	NT	NT	19	8	2.48

^a Values are reported as geometric means with geometric standard deviations. Number of replicates is in parentheses.

^b Twelve values of <3 nM were not factored into this calculation.

^c Calculated using Marvin and calculator plugin freeware (www.chemaxon.com, ChemAxon Kft, Budapest, Hungary).

Subsequent SAR studies revealed that an imidazole was a preferred replacement for the thiazole. We then sought to leverage the C(5)-C(6) region to gain additional potency. Incorporation of a C(5) substituent led to **5** (Table 1), which contained a pendant amide. It was notable that in the x-ray structure of **5**, Gln36 and Arg52 had folded toward the ligand to participate in hydrogen-bonding interactions that were absent in **4**.

Despite the strong enzyme potency of **5**, the IC₅₀ shifted by at least two orders of magnitude between the enzyme and the HWB assay. We supposed that decreasing the lipophilicity would attenuate this shift. Indeed, substitution with a nitrogen atom at an appropriate location in the A ring (**6**) lessened the enzyme-to-HWB potency shift by approximately an order of magnitude.

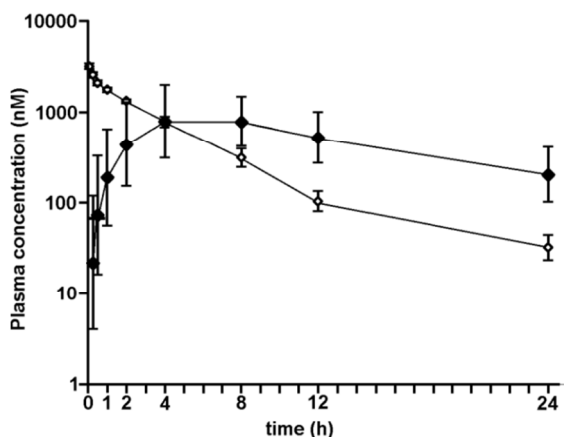
Compounds **5** and **6** had sufficient activity in HWB to be of further interest. In contrast to celecoxib, these analogues suppressed neither PGI₂ formation in the A549 assay nor TXB₂ or PGF_{2 α} production in HWB.³³ Additionally, **8** was at least 10,000-fold selective against COX-1 and COX-2 (no inhibition of either enzyme observed at 10 μ M).³⁴ Taken together, these biochemical outcomes suggested selective inhibition of *m*PGES-1.

1 While neither **5** nor **6** exhibited >50% inhibition at 10 μM in *in vitro* microsomal CYP inhibition as-
2 says, they did display *in vitro* TDI of CYP3A4 at 10 μM . This indicated the potential for DDIs over
3 prolonged dosing, a risk we wished to mitigate.³⁵ It was found that adding a substituent to the imidazole
4 would lower the potential for TDI (see analogues **7–10**.)
5
6
7
8

9
10 Although **7** seemed suitable in many respects, we embarked on further studies aimed at maximizing
11 the activity in HWB. Ultimately, replacement of the distal chlorine with a trifluoromethyl group to fur-
12 nish **8** improved the HWB potency by nearly an order of magnitude. Lower homologues of the isobu-
13 tyramide (**9, 10**) were less potent. Therefore, our interest turned to additional studies of the potency, se-
14 lectivity, and ADME properties of **8**.
15
16
17
18
19
20
21

22 Against *hERG*, **8** had a measurable IC_{50} and K_i (82.6 μM and 41.3 μM , respectively), but the HWB
23 IC_{80} of 69 nM meant that the therapeutic plasma concentration of **8** was likely to be such that a suffi-
24 cient margin should exist between *hERG* activity and *mPGES-1* activity to afford low risk of QT pro-
25 longation.³⁶ Upon testing against a CEREP panel of receptors and ion channels, **8** did not display any
26 activity which would be deemed to present an undue risk.³⁷
27
28
29
30
31
32
33

34 Compound **8** was active in dog whole blood (DWB IC_{50} = 139 nM \times/\div 1.76 and IC_{80} = 703 nM \times/\div
35 2.37 ($n = 16$)). However, in a rat *mPGES-1* enzyme assay, **8** had an IC_{50} of 33.9 μM \times/\div 1.94 ($n = 3$).³⁷
36 This drastic species selectivity was similar to known observations with other classes of *mPGES-1* in-
37 hibitors.³⁸
38
39
40
41
42
43
44



1
2
3
4
5
6
7
8
9
10
11
12
13
14
15
16
17
18
19
20
21
22
23
24
25
26
27
28
29
30
31
32
33
34
35
36
37
38
39
40
41
42
43
44
45
46
47
48
49
50
51
52
53
54
55
56
57
58
59
60

Figure 3. PK of **8** in dog after 2 mg/kg po dosing (solid diamonds, $n = 3$) and 0.5 mg/kg iv dosing (hollow diamonds, $n = 3$). Diamonds indicate geometric means, and error bars represent geometric standard deviations of measured values.

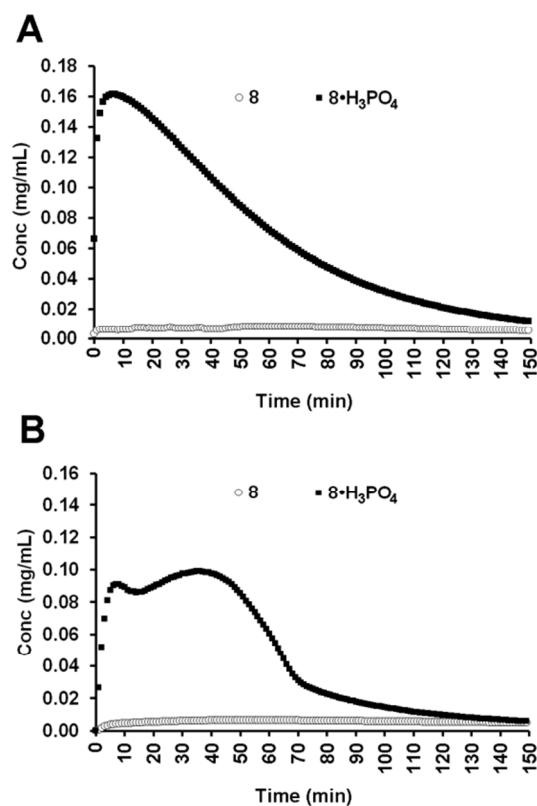


Figure 4. Time-dependent exposure profile of **8** and **8·H₃PO₄** in a dynamic dissolution test in artificial stomach (A) and artificial duodenum (B).

Inhibitor **8** was subjected to a dog PK experiment (Figure 3). The bioavailability was found to be 37%, and at an oral dose of 2 mg/kg, a plasma concentration exceeding 200 nM was sustained for 24 h. This, taken with the known correlation between *ex vivo* IC₈₀ and efficacious plasma concentration,²⁵ gave us pre-clinical evidence even in the absence of a *per se in vivo* efficacy study that a clinically relevant exposure could be achieved at an acceptably low dose.³⁹

1
2
3
4
5
6
7
8
9
10
11
12
13
14
15
16
17
18
19
20
21
22
23
24
25
26
27
28
29
30
31
32
33
34
35
36
37
38
39
40
41
42
43
44
45
46
47
48
49
50
51
52
53
54
55
56
57
58
59
60

However, the slow absorption and low FasSIF solubility of **8** (0.007 mg/mL) prompted us to evaluate enablement options for the compound in order to facilitate dose escalation studies to assess safety without reaching a barrier of dose-limited exposure due to dissolution-limited absorption. While measured thermodynamic solubility in FaSSIF is a valuable initial indicator of the oral absorption potential of compounds, it can sometimes be misleading as it is a result of extended hours of mixing in that medium and not necessarily representative of the *in vivo* gastrointestinal environment. For basic compounds that have a conjugate acid pK_a of approximately 4.5 or greater, it is sometimes possible to enhance dissolution rate through salt formation, and then briefly sustain metastable supersaturation at the site of absorption.⁴⁰ Accordingly, depending on the extent and duration of supersaturation, absorption can be significantly improved.⁴¹

This approach works best for compounds that do not rapidly crystallize and/or precipitate under bio-relevant conditions. From a dynamic dissolution test that mimicked the transfer of orally dosed compound from the stomach to the duodenum,⁴² it was evident that the phosphate salt of **8** had a tendency to dissolve faster than the free base and remain amorphous for an extended period of time (Figure 4). Indeed, *in vivo* PK studies in beagle dog after a 60 mg/kg PO dose showed that **8•H₃PO₄** was more rapidly absorbed than the free base, resulting in higher plasma concentrations and reduced variability at every time point through 24 h (Figure 5). Furthermore, this salt form had acceptable solid state properties. The melting point (190.4 °C), hygroscopicity (<0.5% weight gain when subjected to RH values up to 95%), and physical stability (stable for 2 weeks at 70 °C/75% RH and for 4 weeks at 40 °C/75% RH) all were suitable for development. Therefore, **8•H₃PO₄** was selected as a clinical candidate.

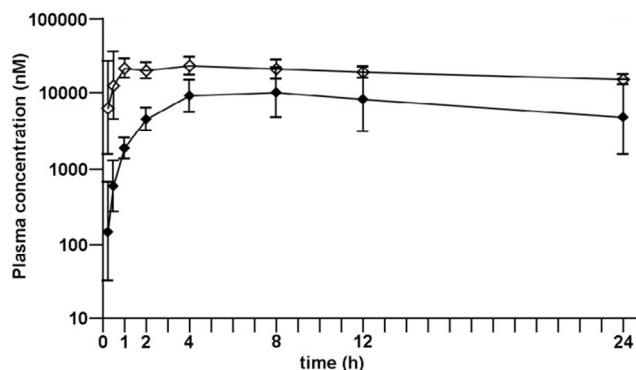
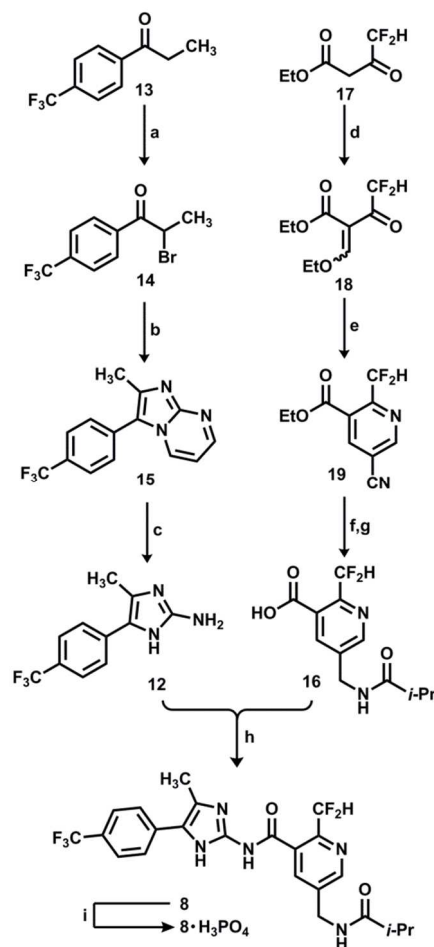


Figure 5. PK of **8** (solid diamonds, $n = 6$) and **8•H₃PO₄** (hollow diamonds, $n = 6$) in dog after 60 mg/kg po dosing. Diamonds indicate geometric means, and error bars represent geometric standard deviations of measured values.

The synthesis of **8•H₃PO₄** was achieved as shown in Scheme 1. Aminoimidazole **12** was prepared by bromination of ketone **13** to give **14**,⁴³ which was cyclized with 2-aminopyrimidine to furnish **15**. This was then subjected to the action of hydroxylamine,⁴⁴ which cleaved the pyrimidine to reveal **12**. The core of **16** was constructed by a modified Hantzsch pyridine synthesis. Condensation of **17**⁴⁵ with triethylorthoformate provided **18**, which was warmed in the presence of 3-dimethylaminoprop-2-enenitrile⁴⁶ to give pyridine **19** after acid-promoted elimination of dimethylamine. Reduction of the nitrile, followed by acylation of the resulting amine and *in situ* saponification of the ester, gave **16**.

Scheme 1. Synthesis of **8•H₃PO₄**^a



^aReagents and conditions: (a) Br₂, AcOH, 92%; (b) 2-aminopyrimidine, NaHCO₃, *i*-PrOH, 80 °C, 22%; (c) NH₂OH, EtOH, 82 °C, 95%; (d) (EtO)₃CH, Ac₂O, 90–100 °C, 86%; (e) (CH₃)₂NCH=CHCN, 60–65 °C, then NH₄OAc, 60–65 °C, 85%; (f) H₂, Pd/C, Boc₂O, EtOH, Et₃N, then HCl, 1,4-dioxane, MTBE, 66%; (g) *i*-PrCOCl, Et₃N, toluene, then LiOH(aq), 70%; (h) T3P, NMM, EtOAc, 65–75 °C, 64%; (i) H₃PO₄, CH₃CN, H₂O, 79%.

To complete the synthesis, **12** and **16** were coupled using T3P to furnish **8**. Generally with unprotected 2-aminoimidazoles, we observed a kinetic preference for acylation of either one of the ring nitrogens *versus* the exocyclic nitrogen, so heating was required to induce isomerization to the N(2)-acylated product. Lastly, **8** was treated with H₃PO₄ to give the phosphate salt.

While **8**·H₃PO₄ was suitable for clinical development, we sought a second molecule with improved physical properties.⁴⁷ We hypothesized that omitting the largely exposed lipophilic ring of **8** would im-

1
2
3
4
5
6
7
8
9
10
11
12
13
14
15
16
17
18
19
20
21
22
23
24
25
26
27
28
29
30
31
32
33
34
35
36
37
38
39
40
41
42
43
44
45
46
47
48
49
50
51
52
53
54
55
56
57
58
59
60

prove solubility, bioavailability, and/or absorption while maintaining the critical hydrogen bonding interactions with the enzyme (Figure 6A). Therefore, we prepared **20** (Table 2). This analogue had only single-digit micromolar potency in our enzyme assay, but it efficiently translated this activity to the *ex vivo* HWB PGE₂ assay. Furthermore, **20** did not demonstrate significant activity in a CYP3A4 TDI assay (20% inhibition after 30 min at 10 μM). Although **20** contained an unsubstituted imidazole, a known risk factor for CYP inhibition,⁴⁸ we reasoned that the lower molecular weight and lipophilicity of **20** *vis-à-vis* analogues **5–10** likely limited the affinity of the former for CYP enzymes.⁴⁹

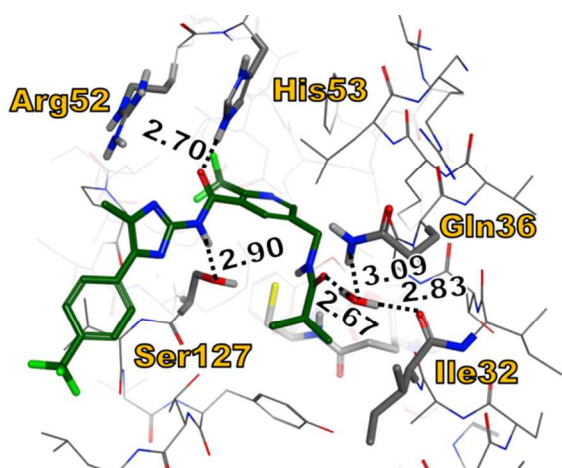
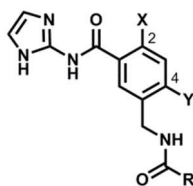


Figure 6. X-ray co-crystal structure of mPGES-1 with **8**. Ligand, key side chains, and glutathione co-factor highlighted with thick bonds. Some atoms omitted for clarity. H-bond distances given in Å.

In rats, **20** was found to be orally bioavailable ($F = 100\%$) and rapidly absorbed ($t_{\max,po} = 15$ min) with low clearance ($CL_{iv} = 26.1$ mL/(min*kg)) and V_{dss} (2.27 L/kg). The efficient translation of enzyme activity to HWB, combined with the PK properties of **20**, encouraged us to pursue an SAR study of these smaller analogues (Table 1).

Increasing the bulk of the amide (**21**, **22**) resulted in a slight potency improvement. In a study of substitution at the C(2) position (**23–26**), halogen atoms proved to be optimal. On the 2-chloro system, further increasing the bulk of the amide provided no potency advantage (**27**). Scaling the benzylic substituent back to an isobutyramide (**28**) reduced potency in the A549 IC₅₀ and HWB IC₈₀ assays, suggesting along with the comparison of **20** and **22** that a pivalamide was optimal. Substitution at the C(4) position tended to decrease potency (**29**, **30**).

Table 2. SAR of Unsubstituted 2-Aminoimidazole *m*PGES-1 Inhibitors.



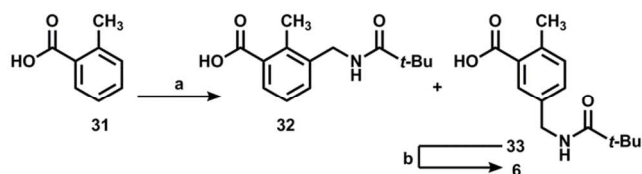
comp d	X	Y	R	<i>m</i> PGES-1 IC ₅₀ ^a	A549 PGE ₂ IC ₅₀ ^a	HWB PGE ₂ IC ₅₀ ^a	HWB PGE ₂ IC ₈₀ ^a	clo gP ^b
20	CF ₂	H	<i>i</i> -Pr	2.46 μM ×/÷	3.15 μM ×/÷	4.61 μM ×/÷ 1.46	31.0 μM ×/÷	2.2
	H	H		1.13 (3)	1.60 (2)	(5)	5.19 (5)	1
21	CF ₂	H	(<i>S</i>)-	1.12 μM ×/÷	8.86 μM ×/÷	10.5 μM ×/÷ 1.08	21.1 μM ×/÷	2.6
	H	H	<i>s</i> - Bu	1.05 (2)	2.18 (2)	(2)	1.08 (2)	5
22	CF ₂	H	<i>t</i> -	0.676 μM ×/÷	3.25 μM ×/÷	1.43 μM ×/÷ 2.08	33.7 μM ×/÷	2.7
	H	H	Bu	1.18 (2)	1.43 (2)	(2)	1.16 (2)	6
23	CF ₃	H	<i>t</i> -	1.08 μM ×/÷	3.23 μM ×/÷	2.14 μM ×/÷ 1.64	10.5 μM ×/÷	3.2
		H	Bu	1.07 (2)	1.50 (2)	(3)	1.93 (3)	5
24	CH ₃	H	<i>t</i> -	3.11 μM ×/÷	4.62 μM ×/÷	2.43 μM ×/÷ 2.47	9.08 μM ×/÷	2.8
		H	Bu	1.35 (2)	2.72 (4)	(3)	1.31 (3)	9

25	Br	H	<i>t</i> - Bu	0.198 μM \times/\div 1.26 (3)	0.284 μM \times/\div 1.52 (2)	0.607 μM \times/\div 1.96 (3)	2.39 μM \times/\div 1.43 (3)	3.1 4
26	Cl	H	<i>t</i> - Bu	0.241 μM \times/\div 1.38 (6)	0.870 μM \times/\div 1.55 (5)	0.744 μM \times/\div 1.46 (6)	2.44 μM \times/\div 1.80 (6)	2.9 8
27	Cl	H	<i>t</i> - Am	0.385 μM \times/\div 1.4 (2)	1.23 μM \times/\div 1.10 (2)	0.853 μM \times/\div 1.50 (3)	9.37 μM \times/\div 1.87 (3)	3.4 1
28	Cl	H	<i>i</i> -Pr	0.885 μM \times/\div 1.32 (2)	2.77 μM \times/\div 1.56 (3)	0.792 μM \times/\div 1.51 (2)	8.80 μM \times/\div 1.34 (2)	2.4 2
29	Cl	CH 3	<i>i</i> -Pr	2.32 μM \times/\div 1.14 (2)	8.85 μM \times/\div 1.13 (2)	13.0 μM \times/\div 1.69 (3)	132 μM \times/\div 2.13 (3)	2.9 4
30	Cl	F	<i>i</i> -Pr	3.67 μM \times/\div 1.03 (2)	>10 μM (2)	9.53 μM \times/\div 1.89 (3)	57.4 μM \times/\div 4.29 (3)	2.5 7

^a Values are reported as geometric means with geometric standard deviations. Number of replicates is in parentheses.

^b Calculated using Marvin and calculator plugin freeware (www.chemaxon.com, ChemAxon Kft, Budapest, Hungary).

None of the analogues **20–30** decreased PGI₂ production in A549 cells up to 10 μM or PGF_{2 α} or TXB₂ production in HWB up to 30 μM , suggesting that these compounds did not have COX inhibitory activity.³³ Indeed, compound **26** was inactive against COX-1 and COX-2 (9% inhibition at 100 μM and 16% at 30 μM , respectively).³⁴ Therefore, it was concluded that the PGE₂ reduction exhibited by **26** resulted from selective *m*PGES-1 inhibition.

Scheme 2. Synthesis of **24**.^a

^aReagents and conditions: (a) *t*-BuCONHCH₂OH, H₂SO₄, rt, then chromatographic separation, 27% of **32** and 28% of **33**; (b) 2-aminoimidazole monosulfate, BOP, Et₃N, DMF, 60 °C, 87%.

For this SAR study, most cores which were not commercially available could be prepared by Tscherniac-Einhorn alkylation.^{50,51} For example, *o*-toluic acid (**31**, Scheme 2) was treated with *N*-(hydroxymethyl)pivalamide in the presence of sulfuric acid to furnish a separable mixture of **32** and **33**, and then **33** was carried forward to **24**. Although this chemistry was not regioselective, it enabled facile exploration of C(2) and C(4) substituents by providing rapid access to the requisite functionalized benzoic acids.

Of the analogues in Table 2, **25** and **26** had the lowest HWB IC₈₀ values. Between these two compounds, **26** had the lower molecular weight and *clogP*, so it was selected for further evaluation.

Against *h*ERG, **26** had no significant measurable activity (−4% and 14% inhibition at 10 μM and 100 μM, respectively). However, the decreased *m*PGES potency of **26** and the high *h*ERG IC₅₀ of **8** prevented a meaningful comparison between **8** and **26** in this regard. However, on the basis of these data, **26** was not expected to carry a significant QT prolongation risk. Compound **26** did not display any significant activity against a CEREP panel of receptors and ion channels.³⁷

Similarly to **8**, compound **26** was active in dog whole blood (DWB IC₅₀ = 0.555 μM ×/÷ 1.90 and IC₈₀ = 1.84 μM ×/÷ 2.06 (*n* = 5)) but had substantially less potency in the rat *m*PGES-1 assay (IC₅₀ >1000 μM) than in the human enzyme assay. With the potential to use the dog as an on-target species, we studied the PK properties of **26** in dog (Figure 6).

In dogs, it was found that **26** was readily orally bioavailable when administered as an aqueous suspension of crystalline material ($F = 60\% \times/\div 1.17$ after 0.5 mg/kg po and iv dosing, Figure 7A).

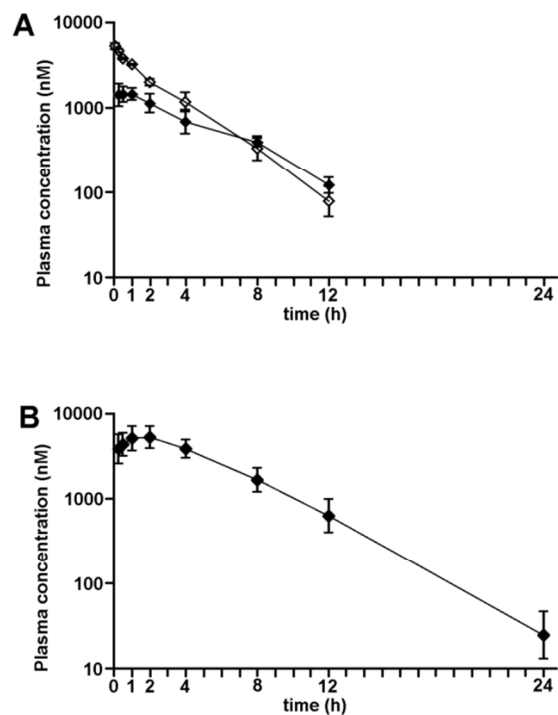
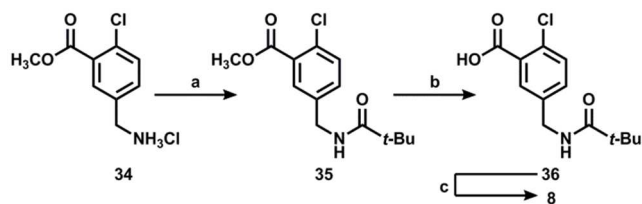


Figure 7. PK of **26** in dog (A) after 0.5 mg/kg po dosing (solid diamonds, $n = 3$) and 0.5 mg/kg iv dosing (hollow diamonds, $n = 3$) and (B) after 2 mg/kg po dosing ($n = 3$). Diamonds indicate geometric means, and error bars represent geometric standard deviations of measured values.

After a 2 mg/kg po dose (Figure 7B), plasma concentrations exceeding 1 μM were achieved in less than 15 minutes and sustained for at least 8 hours. Compound **26** exhibited relatively little exposure variability between animals; the geometric SD for plasma concentration was ≤ 2.0 at all timepoints in both dog PK studies. The desirable PK properties of **26**, along with its potency in HWB and selectivity for *m*PGES-1, informed us in our selection of **26** as a clinical candidate.³⁷ It was notable that the supe-

rior physicochemical properties and reduced exposure variability of **26** compared to **8** sufficiently compensated for reduced potency to make **26** a viable molecule to test in the clinic.⁴⁷

Scheme 3. Synthesis of **26**.^a



^aReagents and conditions: (a) *t*-BuCOCl, DIEA, CH₂Cl₂, rt, 1 h; (b) LiOH, H₂O, 1,4-dioxane, rt, 1 h, then HCl_(aq), 97% (2 steps); (c) 2-aminoimidazole monosulfate, TBTU, DIEA, DMF, 80 °C, 18 h, 83%.

A larger-scale synthesis of **26** proceeded straightforwardly from commercially available **34** (Scheme 3).⁵² Acylation of the amine with pivaloyl chloride furnished **35**. Saponification of the crude ester gave **36**, which was coupled with 2-aminoimidazole with heating to furnish **26** in *ca.* 81% yield over three steps. We viewed the simplicity of this synthesis as a potential advantage for the development of **26**.

CONCLUSION

SAR efforts guided by structural insights yielded two clinical candidates, **8**•H₃PO₄ and **26**, with different profiles. While **8**•H₃PO₄ was significantly more potent in the enzyme and HWB assays, **26** had an improved pharmacokinetic profile in dog while still exhibiting a HWB IC₅₀ for PGE₂ suppression comparable to that of celecoxib. Based on the known PK/PD relationship with COX-2 inhibitors, this pair of compounds was expected to offer insight into the validity of *m*PGES-1 inhibition as a mechanism for analgesia in human patients.

EXPERIMENTAL SECTION

General Methods. All reagents and anhydrous solvents were obtained from commercial sources and used without further purification unless noted otherwise. ¹H NMR spectra were recorded on a Bruker 300 MHz spectrometer, a Bruker 400 MHz spectrometer, a Bruker 500 MHz spectrometer, or a Varian 400 MHz spectrometer. ¹H NMR chemical shifts are reported in ppm with the solvent as the internal

1 standard (DMSO-*d*₅ 2.49 ppm, CHCl₃ 7.26 ppm). ¹³C NMR chemical shifts are reported in ppm with
2 the solvent as the internal standard (DMSO-*d*₆ 39.52 ppm). ¹⁹F NMR chemical shifts are reported in
3 ppm relative to an external standard of CFCl₃. ³¹P NMR chemical shifts are reported in ppm relative to
4 an external standard of 85% H₃PO₄.
5
6
7
8

9
10 Compounds were analyzed for purity by HPLC and HPLC-MS, and unless otherwise stated, purities
11 of synthesized compounds were all found to be >95% by the following HPLC method:
12
13

14 Agilent 1100 HPLC with VWD detectors, Waters Exterra MS 4.6 mm × 150 mm × 3.5 μm C₁₈ col-
15 umn; Eluent: 0.1% formic acid in a gradient of 5% to 100% CH₃CN in water over 3.75 min; Flow rate
16 1.0 mL/min; Column temp. 50 °C; λ 300 nm and 214 nm.
17
18
19
20
21

22 **2-bromo-1-(4-(trifluoromethyl)phenyl)-1-propanone (14).** At room temperature, a mixture of 4-
23 (trifluoromethyl)propiophenone (**13**, 100 g, 494 mmol) and glacial acetic acid (200 mL) was treated
24 with a solution of bromine (79 g, 494 mmol) in glacial acetic acid (200 mL) over the course of 60
25 minutes. After the end of the addition, the mixture was stirred for 1.5 hours, then was quenched with
26 cold water (<5 °C, 1.2 L) and stirred for 3 hours at between 0 °C and 5 °C. The resulting slurry was fil-
27 tered and washed with water (10 °C–15 °C, 1 L), and dried under reduced pressure at between 25 °C
28 and 30 °C for 15 hours to furnish **14** (128.1 g, 92% yield). ¹H NMR (400 MHz, CDCl₃): δ 8.13 (d, *J* =
29 8.3 Hz, 2H), 7.76 (d, *J* = 8.3 Hz, 2H), 5.26 (q, *J* = 6.7 Hz, 1H), 1.93 (d, *J* = 6.3 Hz, 2H).
30
31
32
33
34
35
36
37
38
39
40
41
42
43

44 **2-methyl-3-(4-(trifluoromethyl)phenyl)imidazo[1,2-*a*]pyrimidine (15).** A mixture of **14** (100 g,
45 356 mmol), 2-aminopyrimidine (33.9 g, 356 mmol), NaHCO₃ (59.8 g, 811 mmol), and toluene (500
46 mL) was heated to between 90 °C and 100 °C for 24 hours with stirring. The mixture was cooled to be-
47 tween 40 °C and 45 °C, and the product was isolated by vacuum distillation. The distillate was cooled
48 to between 25 °C and 30 °C, treated with water (1 L), and stirred for 4 h. The solids were collected by
49 filtration, washed with a 9:1 (v/v) mixture of hexanes and MTBE (200 mL), and dried in a vacuum oven
50 at between 45 °C and 50 °C to furnish **15** (35.4 g, 35% yield). ¹H NMR (400 MHz, DMSO-*d*₆): δ 8.86
51
52
53
54
55
56
57
58
59
60

1 (dd, $J = 6.9, 1.9$ Hz, 1H), 8.56 (dd, $J = 4.2, 2.0$ Hz, 1H), 8.07 (d, $J = 8.8$ Hz, 2H), 7.84 (d, $J = 8.7$ Hz,
2 2H), 7.11 (dd, $J = 6.9, 4.0$ Hz, 1H), 2.69 (s, 3H). LC/MS (ESI⁺): (m/z) 278 (M+H)⁺.
3
4

5 **4-methyl-5-(4-(trifluoromethyl)phenyl)-1H-imidazol-2-amine (12)**. A mixture of **15** (180 g, 649
6 mmol), EtOH (1.4 L), and hydroxylamine (159 mL, 2.60 mol) was stirred at 82 °C for 48 hours, then
7 cooled and concentrated to dryness. The residue was diluted with CH₂Cl₂ (1.5 L) and washed with wa-
8 ter (2 × 500 mL) and saturated aqueous NaCl (500 mL). The organic phase was dried over MgSO₄, fil-
9 tered, and concentrated under reduced pressure to give a yellow gum. This was subjected to flash
10 chromatography on silica gel, eluting with a gradient of 0% to 25% (2% NH₃ in CH₃OH) in CH₂Cl₂, to
11 furnish **12** as a yellow foam (150.3 g, 96% yield). ¹H NMR (300 MHz, CDCl₃): δ 7.42 (ABq, $J_{AB} = 8.9$
12 Hz, $\Delta\delta_{AB} = 0.058$, 4H), 6.48 (v br s, 3H), 2.16 (s, 3H). LC/MS (ESI⁺): (m/z) 242 (M+H)⁺.
13
14
15
16
17
18
19
20
21
22
23

24 **2-(difluoromethyl)-5-(isobutyramidomethyl)-N-(4-methyl-5-(4-(trifluoromethyl)phenyl)-1H-**
25 **imidazol-2-yl)nicotinamide (8)**. A mixture of **16** (230 g, 845 mmol), **12** (281 g, 845 mmol), NMM
26 (428 g, 4.22 mol), and EtOAc (2.5 L) was stirred between 15 °C and 25 °C for 1 h, then treated with
27 propylphosphonic anhydride (50% w/w in EtOAc, 1.88 kg, 2.95 mol) over the course of 17 minutes,
28 maintaining the internal temperature below 40 °C. The addition vessel was rinsed with EtOAc (415
29 mL), which was added to the reaction vessel. The mixture was stirred for one additional hour, then was
30 warmed to between 65 °C and 75 °C with stirring overnight. The mixture was cooled to between 15 °C
31 and 25 °C and diluted with EtOAc, then washed with water (2 × 2 L), 1 N aqueous HCl (2 × 2 L), satu-
32 rated aqueous NaCl (2 × 2 L), 10% (w/w) aqueous Na₂CO₃ (2 × 2 L), then deionized water (2 × 2 L).
33 The organic phase was concentrated under reduced pressure until solids appeared (at a volume of *ca.* 4
34 L), then absolute EtOH (3 L) was added, and the mixture was concentrated to a volume of *ca.* 3 L. Ab-
35 solute EtOH (1 L) was added, and the mixture was stirred at between 65 °C and 75 °C for 30 min, then
36 at between 15 °C and 25 °C for 63 hours. The slurry was cooled to between -5 °C and -15 °C with stir-
37 ring for two hours, then the solids were isolated by filtration, rinsed with cold (-10 °C) absolute EtOH
38 (420 mL), and dried in a 50 °C vacuum oven for two nights to furnish **8** (268 g, 64% yield). ¹H NMR
39
40
41
42
43
44
45
46
47
48
49
50
51
52
53
54
55
56
57
58
59
60

(400 MHz, DMSO- d_6): δ 12.08 (br s, 2H), 8.65 (s, 1H), 8.40 (t, $J = 5.6$ Hz, 1H), 8.06 (s, 1H), 7.81 (A of ABq, d, $J = 8.1$ Hz, 2H), 7.73 (B of ABq, d, $J = 8.1$ Hz, 2H), 7.35 (v br t, $J = 54$ Hz, 1H), 4.38 (d, $J = 5.6$ Hz, 2H), 2.46 (s, 3H), 2.44 (septet, $J = 6.8$ Hz, 1H), 1.04 (d, $J = 6.8$ Hz, 6H). $^{13}\text{C}\{^1\text{H}\}$ NMR (100 MHz, DMSO- d_6): δ 176.4, 165.5, 149.4, 147.7 (t, $J = 22.0$ Hz), 141.1 (br s), 138.1 (br s), 137.1, 135.8, 130.7 (br s), 125.9 (q, $J = 31.9$ Hz), 125.7, 125.4 (q, $J = 3.7$ Hz), 124.5 (q, $J = 271.4$ Hz), 122.3 (br s), 111.5 (t, $J = 238.4$ Hz), 34.0, 19.5, 11.2. $^{19}\text{F}\{^1\text{H}\}$ NMR (376.5 MHz, DMSO- d_6): δ -60.7, -115.0. ^{31}P NMR (400 MHz, DMSO- d_6): no signal. LC/MS (ESI $^+$): (m/z) 496 (M+H) $^+$, 518 (M+Na) $^+$, 534 (M+K) $^+$. HRMS calcd for C₂₃H₂₃F₅N₅O₂ (M+H) $^+$: 496.1772, found 496.1771. Anal. calcd. for C₂₃H₂₂F₅N₅O₂: C, 55.75; H, 4.48; N, 14.14; found: C, 55.53; H, 4.43; N, 14.11.

2-(difluoromethyl)-5-(isobutyramidomethyl)-N-(4-methyl-5-(4-(trifluoromethyl)phenyl)-1H-imidazol-2-yl)nicotinamide phosphoric acid salt (8•H₃PO₄). To a mixture of **8** (250 g, 505 mmol) in CH₃CN (5 L) was added a solution of 85% H₃PO₄ (110.7 g, 960 mmol) in deionized water (1 L). The mixture was heated to between 60 °C and 70 °C, then filtered through a 1.2 μM filter capsule. The filtrate was heated to between 55 °C and 65 °C, then was stirred at ambient temperature overnight. The mixture was cooled to 5 °C and stirred at that temperature for 2 hours. The resulting solids were collected by filtration and rinsed with cold (0 °C–10 °C) CH₃CN (2 \times 475 mL), followed by cold (0 °C–10 °C) deionized water (2 \times 475 mL). The wet solids were slurried with deionized water (2.5 L) at room temperature for 2 hours, then collected by filtration and rinsed with the filtrate (3 \times), followed by deionized water (1.25 L). The solids were dried at 110 °C under reduced pressure to furnish **8•H₃PO₄** as a pale yellow solid (237 g, 79% yield). ^1H NMR (400 MHz, DMSO- d_6): δ 8.65 (d, $J = 1.8$ Hz, 1H), 8.42 (t, $J = 5.8$ Hz, 1H), 8.06 (s, 1H), 7.81 (A of ABq, d, $J = 8.1$ Hz, 2H), 7.73 (B of ABq, d, $J = 8.1$ Hz, 2H), 7.35 (t, $J = 54.1$ Hz, 1H), 4.38 (d, $J = 5.6$ Hz, 2H), 2.46 (s, 3H), 2.45 (septet, $J = 6.9$ Hz, 1H), 1.04 (d, $J = 6.9$ Hz, 6H). $^{13}\text{C}\{^1\text{H}\}$ NMR (100 MHz, DMSO- d_6): δ 176.5, 165.5, 149.5, 147.7 (t, $J = 22.0$ Hz), 141.1, 137.9, 137.2, 135.8, 130.7 (t, $J = 3.7$ Hz), 127.6, 126.1, 125.9 (q, $J = 31.9$ Hz), 125.4 (q, $J = 3.7$ Hz), 124.5 (q, $J = 271.4$ Hz), 122.4, 111.5 (t, $J = 238.4$ Hz), 34.0, 19.5, 11.2. $^{19}\text{F}\{^1\text{H}\}$ NMR (376.5

1
2
3
4
5
6
7
8
9
10
11
12
13
14
15
16
17
18
19
20
21
22
23
24
25
26
27
28
29
30
31
32
33
34
35
36
37
38
39
40
41
42
43
44
45
46
47
48
49
50
51
52
53
54
55
56
57
58
59
60

MHz, DMSO-*d*₆): δ -60.7, -115.0. ³¹P NMR (400 MHz, DMSO-*d*₆): δ -0.7. HRMS calcd for C₂₃H₂₃F₅N₅O₂ (M)⁺: 496.1772, found 496.1755. Anal. calcd. for C₂₃H₂₄F₅N₅O₆P: C, 46.55; H, 4.25; F, 16.01; N, 11.80; found: C, 46.63; H, 4.22; F, 16.30; N, 11.91.

2-chloro-5-(pivalamidomethyl)benzoic acid (36). A thermally controlled reactor was charged with methyl 5-(aminomethyl)-2-chlorobenzoate hydrochloride (**34**, 700 g, 2.96 mol), dichloromethane (4.90 L), and *N,N*-diisopropylethylamine (1.45 L, 8.30 mol). Pivaloyl chloride (436 mL, 3.56 mol) was added at such a rate that the internal temperature did not rise above 21 °C. The resulting solution was stirred at room temperature for 1 h. Then, the mixture was quenched with saturated aqueous NaHCO₃ (10 L) and extracted with dichloromethane (2 × 1000 mL). The combined organic extracts were dried over sodium sulfate and filtered. The filtrate was concentrated under reduced pressure to furnish crude **35** as a straw-colored oil. This was dissolved in 1,4-dioxane (5.25 L) and treated with water (3.15 L) and LiOH·H₂O (408 g, 9.62 mol) and stirred at room temperature for 1 h. The mixture was then treated with 5.0 M aqueous HCl (3 L) (*Caution! Exotherm!*) and concentrated under reduced pressure to remove *ca.* 6 L of volatile material. The resulting suspension was cooled to 10 °C, and the solids were isolated by filtration, washed with water (8 L), and dried on the sinter for 3 h. The solids were then dried in a 40 °C vacuum oven for 48 hours to furnish **36** as a free-flowing white solid (775 g, 97% yield over two steps). ¹H NMR (400 MHz, DMSO-*d*₆): δ 13.32 (s, 1H), 8.13 (t, *J* = 5.8 Hz, 1H), 7.62 (d, *J* = 2.4 Hz, 1H), 7.47 (d, *J* = 8.3 Hz, 1H), 7.34 (dd, *J* = 8.3, 2.0 Hz, 1H), 4.25 (d, *J* = 5.8 Hz, 2H), 1.11 (s, 9H). LC/MS (ESI⁺): (*m/z*) (³⁵Cl/³⁷Cl) 270/272 (M+H)⁺.

2-chloro-*N*-(1H-imidazol-2-yl)-5-(pivalamidomethyl)benzamide (26). A thermally controlled reaction vessel containing **36** (420 g, 1.56 mol), 2-aminoimidazole monosulfate (349 g, 1.87 mol), and DMF (2.94 L) was treated with *o*-benzotriazol-1-yl-*N,N,N',N'*-tetramethyluronium tetrafluoroborate (722 g, 2.18 mol) and then DIEA (869 mL, 4.98 mol) and heated to an internal temperature of 80 °C for 18 h. Then, the reaction mixture was cooled to 10 °C and added to ice water (14 L) and stirred for 90 min. The resulting solids were collected by filtration and air dried for 24 h, then dried further in a 50 °C vac-

uum oven for 24 h. The resulting solid material was slurried in isopropanol (7 L), heated to an internal temperature of 73 °C for 3 h, cooled to 10 °C, and the solids were isolated by filtration. The resulting material was air dried for 24 h, then dried further in a 55 °C vacuum oven for 48 h to furnish **26** as a fine, off-white solid (435 g, 83% yield). ¹H NMR (400 MHz, DMSO-*d*₆): δ 11.83 (br s, 2H), 8.12 (t, *J* = 6.0 Hz, 1H), 7.46 (d, *J* = 8.3 Hz, 1H), 7.39 (d, *J* = 1.7 Hz, 1H), 7.30 (dd, *J* = 8.3, 2.0 Hz, 1H), 6.72 (br s, 2H), 4.26 (d, *J* = 5.9 Hz, 2H), 1.11 (s, 9H). ¹³C{¹H} NMR (100 MHz, DMSO-*d*₆): δ 177.6, 165.6, 141.3, 139.5, 135.7, 129.6, 129.5, 128.1, 127.6, 118.1 (v br s), 41.4, 38.0, 27.4. LC/MS (ESI⁺): (*m/z*) (³⁵Cl/³⁷Cl) 335/337 (M+H)⁺. HRMS calcd. for C₁₆H₂₀ClN₄O₂ (M+H)⁺: 335.1275, found 335.1274. Anal. calcd. for C₁₆H₁₉ClN₄O₂: C, 57.40; H, 5.72; N, 16.73; Cl, 10.59; O, 9.56; found: C, 57.27; H, 5.64; N, 16.79; Cl, 10.59, O, 9.57.

Biological Assays.

***m*PGES-1 Enzyme Inhibition Assays.** Human or rat *m*PGES-1 (InvitrogenTM (Cat #97002RG, clone ID 6374722)) was subcloned into pcDNATM3.1 and transiently expressed in 293E cells. Microsomes were prepared from cell pellets based on published methods.^{10,11} Pellets were brought up in homogenization buffer (15 mM Tris-HCl, pH 8.0; 0.25 M sucrose; 0.1 mM EDTA; 1 mM glutathione) and sonicated 5 × 30 seconds on ice. Homogenate was centrifuged at 5000g for 10 minutes at 4 °C. The supernatant fraction was decanted, loaded into Beckman Quick-Seal[®] tubes, and centrifuged at 150000g for 90 minutes at 4 °C. The supernatant fraction was discarded by decantation, and the pellets were resuspended in assay buffer (10 mM sodium phosphate (pH 7.0), 10% glycerol, and 2.5 mM glutathione Complete Protease Inhibitor Cocktail (Roche)). Protein concentration was determined using the Pierce Coomassie PlusTM reagent.

For the enzyme assay, the microsomes were diluted into assay buffer and 14 μL/well was added to 384 well plates. Compound dilution plates (Nunc[®] Catalog #249944) were generated on a Tecan EvoTM, and 4 μL/well was added to the assay plates. PGH₂ was diluted into assay buffer immediately prior to use, and 7 μL/well was added. Final concentrations were 6.52 μg/mL of microsomes and 1.67 μM PGH₂.

1 After a 2.5 minute incubation at room temperature, 5 μL /well of (1 mg/mL of SnCl_2 in 0.5 N $\text{HCl}_{(\text{aq})}$)
2 was added to stop the reaction. 5 μL of the reaction was transferred to a 384 well plate containing 0.1%
3 aqueous formic acid (45 μL) for Mass Spec dilution, then the plates were stored at $-20\text{ }^\circ\text{C}$. The plates
4 were analyzed for PGE_2 using standard LC/MS/MS analysis (Biocius Lifesciences, Wakefield, MA,
5 USA).
6
7
8
9
10

11 **Cell-Based Assay.** Human epithelial lung carcinoma cell line A549 was purchased from ATCC (CCL-
12 185) and was maintained in Kaighn's F12 + 10% FBS, 5% CO_2 . For the assay, cells were plated at
13 40,000/well in 96-well Falcon plates, 24 hours prior to treatment. Compounds were diluted in DMSO
14 and were added at 1 μL /well, $n=2$, to give seven concentrations each. Cells were pretreated 30 minutes
15 at $37\text{ }^\circ\text{C}$, 5% CO_2 . rhIL-1 β (R&D Systems) was added to give 0.2 ng/mL final. The treatment period
16 was ~ 18 hours. The conditioned medium was assayed for levels of PGE_2 and 6-keto $\text{PGF}_{1\alpha}$ by EIA
17 (Cayman). The IC_{50} s were calculated using Graphpad Prism nonlinear regression sigmoidal dose re-
18 sponse curve fitting. Data are the geometric mean \times/\pm geometric standard deviation of the indicated
19 number of determinations.
20
21
22
23
24
25
26
27
28
29
30
31
32

33 **Human Whole Blood Assay.** With informed consent, blood was collected from normal volunteer do-
34 nors into sodium heparin vacutainer tubes. Donors had not taken NSAIDs, aspirin, celecoxib, or gluco-
35 corticoids within two weeks of the donation. All tubes from each donor were pooled into 250 mL Corn-
36 ing conical centrifuge tubes and 436.5 μL /well was distributed into deep well polypropylene plates.
37 Test compounds were diluted in DMSO to $100\times$ the final concentration, and 4.5 μL /well in duplicate or
38 triplicate was added to give 7 point curves. The blood was pretreated at $37\text{ }^\circ\text{C}$, 5% CO_2 , in a humidified
39 atmosphere, loosely covered with a silicone cap mat, for 30 minutes, after which 9 μL /well of a solution
40 of 5 mg/mL of lipopolysaccharide (LPS) (Sigma 0111:B4) in 1 mg/mL bovine serum albumin
41 (BSA)/PBS was added to give a final LPS concentration of 100 $\mu\text{g}/\text{mL}$. The plates were incubated for
42 20–24 hours, loosely covered, at $37\text{ }^\circ\text{C}$, 5% CO_2 , in a humidified atmosphere, on an orbital shaker at
43 approximately 100 rpm. The plates were tightly sealed with silicone cap mats and chilled on ice for ap-
44
45
46
47
48
49
50
51
52
53
54
55
56
57
58
59
60

1 proximately 1 hour. Then, the plates were centrifuged at 1800g for 10 minutes at 4 °C in an Eppendorf
2 5810R centrifuge. Plasma was removed from the cell layer using the Rainin L200 with sterile filtered
3 tips and transferred to v-bottom polypropylene plates. 100 µL was quantitatively transferred to Costar
4 cluster tubes blocks; and 400 µL/well of the methanol stop reagent and of each of the internal standards
5 PGE₂-d₄, PGF_{2α}-d₄, and TXB_{2β}-d₄ were added. Samples were vortexed for 5 minutes and placed at -20
6 °C for at least one hour. Samples were centrifuged for 10 minutes at 4000 rpm in an Eppendorf 5810R.
7
8
9
10
11
12
13

14 Solid phase extraction was performed using Waters HLB 30 mg/bed 96 well plates on a vacuum mani-
15 fold: 1) the matrix was washed with methanol (1 mL), followed by 0.1% formic acid in water (1 mL); 2)
16 400 µL sample was applied along with 0.1% formic acid in water (900 µL) and allowed to bind for 5
17 minutes; 3) the matrix was washed with 0.1% formic acid in water (600 µL), followed by 80/20 wa-
18 ter/methanol (600 µL); 4) the products were eluted with EtOAc (2 × 500 µL); 5) the samples were dried
19 under nitrogen and reconstituted in 75/25 water/acetonitrile with 0.1% formic acid (50 µL). The prod-
20 ucts were analyzed by LC-MS/MS.
21
22
23
24
25
26
27
28
29
30

31 **Dog Whole Blood Assay.** Dog whole blood was obtained from Covance (Greenfield, Indiana). All
32 tubes from each donor were pooled and kept on ice. To 96-well Falcon 3072 plates, 98 µL of blood was
33 added per well. Test compounds were diluted in DMSO to 100× the final concentration, and 1 µL/well
34 in duplicate or triplicate was added to each well to give 7 point curves. The blood was pretreated with
35 compounds at 37 °C, 5% CO₂, in a humidified atmosphere for 30 minutes, after which 1 µL/well of a
36 solution of 0.1 mg/mL of lipopolysaccharide (LPS) (Sigma, serotype 0111:B4) in 0.1% bovine serum
37 albumin (BSA)/PBS was added to give a final LPS concentration of 1 µg/mL. The plates were incubat-
38 ed for 5 hours at 37 °C, 5% CO₂, in a humidified atmosphere. After incubation, the plates were chilled
39 on ice for approximately 10 min. Then, the plates were centrifuged at 1800g for 10 minutes at 4 °C in
40 an Eppendorf 5810R centrifuge. Plasma was removed from the cell layer and transferred to v-bottom
41 polypropylene plates. Plasma samples were assayed for PGE₂ at 1:50 dilution using PGE₂ Express EIA
42 assay kit (Cayman Chemical). The plates were read at A₄₁₂ on a plate reader (Molecular Devices Versa-
43
44
45
46
47
48
49
50
51
52
53
54
55
56
57
58
59
60

1 max) using SOFTmaxPRO (v. 4.3.1) software. IC₅₀ values were calculated using Graphpad Prism non-
2 linear regression, sigmoidal dose response curve fitting.
3

4
5 **CYP 3A4 Inhibition Assay.** Incubation samples were prepared by adding 150 μL of a solution of mi-
6 crosomes (protein concentration 66.8 μg/mL, adjusted to pH 7.4 with phosphate buffer) and 2 μL of a 1
7 mM (90:10 CH₃CN:DMSO) solution of test compound, and mixed well. Samples were pre-incubated
8 for approximately 10 minutes at approximately 37 °C. Following the pre-incubation period, the reaction
9 was initiated with the addition of 50 μL of a solution of NADPH (2 mM), containing marker substrates
10 bufuralol (40 μM), midazolam (20 μM), and diclofenac (40 μM) in Milli-Q water. Final incubation vol-
11 ume was 200 μL, which contained 10 μM test compound, 10 μM bufuralol, 5 μM midazolam, 10 μM
12 diclofenac, 0.5 mM NADPH, and 0.05 mg/mL protein.
13
14

15
16
17
18
19
20
21
22
23
24
25
26
27
28
29
30
31
32
33
34
35
36
37
38
39
40
41
42
43
44
45
46
47
48
49
50
51
52
53
54
55
56
57
58
59
60
The reaction mixture was incubated for 3 minutes at approximately 37 °C, after which a 70 μL aliquot
was taken from the reaction mixture and quenched by addition to 60 μL of an acetonitrile solution con-
taining 1-hydroxybufuralol maleate-*d*₉ (0.12 μM), α-hydroxymidazolam-*d*₄ (0.17 μM) and [¹³C₆]-4'-
hydroxydiclofenac (0.19 μM). The reaction mixture was centrifuged at approximately 4000 rpm for 15
minutes at approximately 5 °C. Following centrifugation, the samples were analyzed by LC-MS/MS
using the following method:

LC Column: Javelin Betasil C₁₈ (20 mm × 2 mm); Mobile Phase A: 98.5:1:0.5 Milli-Q H₂O : CH₃OH:
1 M NH₄HCO₃ (v/v); Mobile Phase B: 99:1 CH₃OH: 1 M NH₄HCO₃ (v/v). Stepwise gradient from
98% Mobile Phase A/2% Mobile Phase B to 2% Mobile Phase A/98% Mobile Phase B over 0.85
minutes.

MS/MS method: Collision gas: 10 psi; Curtain gas: 40 psi; Ion source gas 1: 55 psi; Ion source gas 2:
70 psi; IonSpray voltage: 1500 V; Source temperature: 700 °C; Entrance potential: 10 V. Samples were
analyzed for metabolites and internal standards with their respective mass transitions 1-OH-bufuralol
(278.1/186.1), 1-OH-bufuralol-*d*₉ (287.1/186.1), 1-OH-midazolam (342.1/203.1), 1-OH-midazolam-*d*₄
(346.1/203.1), 4-OH-diclofenac (312.2/231.2), and 4-OH-diclofenac-*d*₆ (318.2/231.2). Area ratios (me-

1 tabolite area / stable label metabolite internal standard) were determined for incubations with inhibitor
2 and compared with incubations containing solvent only (vehicle control). Percent inhibition was calcu-
3 lated by $100 - (\text{area ratio with test compound} / \text{area ratio vehicle control} \times 100)$.
4
5
6

7 **CYP 3A4 Time-Dependent Inhibition Assay.** Incubation samples were prepared by adding 178 μL
8 of a solution of microsomes (protein concentration 56.18 $\mu\text{g}/\text{mL}$, adjusted to pH 7.4 with phosphate
9 buffer) and mixing well. These were pre-incubated for approximately 12 minutes at approximately 37
10 $^{\circ}\text{C}$. Following the pre-incubation period, the inactivation reaction was initiated with the addition of 2
11 μL of a 1 mM (90:10 $\text{CH}_3\text{CN}:\text{DMSO}$) solution of inhibitor and 20 μL of a solution of NADPH (10 mM)
12 in a pH 7.4 aqueous (100 mM) phosphate buffer to give a final concentration of 10 μM test compound, 1
13 mM NADPH, and 0.5 mg/mL microsomes.
14
15
16
17
18
19
20
21
22
23

24 Separately, two activity plates (one each for a 0-minute and a 30-minute time point) were prepared
25 containing 95 μL of a solution of NADPH (1 mM) and midazolam (100 μM) in a pH 7.4 aqueous (100
26 mM) phosphate buffer, and pre-incubated at 37 $^{\circ}\text{C}$ for approximately 12 minutes. These were called
27 Plate 0 and Plate 30, respectively.
28
29
30
31
32
33

34 Immediately upon preparation of the inactivation sample, a 5 μL aliquot was taken and added to Plate
35 0 and incubated at 37 $^{\circ}\text{C}$ for 1 minute. This was quenched by the addition of 50 μL of an acetonitrile
36 solution of α -hydroxymidazolam- d_4 (0.17 μM).
37
38
39
40

41 After incubating for 30 minutes, a 5 μL aliquot of the inactivation sample was taken and added to
42 Plate 30 and incubated at 37 $^{\circ}\text{C}$ for 1 minute. This was quenched by the addition of 50 μL of an ace-
43 tonitrile solution of α -hydroxymidazolam- d_4 (0.17 μM).
44
45
46
47
48

49 The reaction mixtures were centrifuged at approximately 4000 rpm for 15 minutes at approximately 5
50 $^{\circ}\text{C}$. Following centrifugation, the samples were analyzed by LC-MS/MS using the following method:
51
52

53 LC Column: Javelin Betasil C_{18} (20 mm \times 2 mm); Mobile Phase A: 95:5 Milli-Q H_2O : 1 M
54 NH_4HCO_3 (v/v); Mobile Phase B: 95:5 CH_3OH : 1 M NH_4HCO_3 (v/v). Gradient: 0.3 min at 95:5 Mobile
55
56
57
58
59
60

1 Phase A:Mobile Phase B; ramp to 5:95 Mobile Phase A:Mobile Phase B over 1.0 minute; hold at 5:95
2
3 Mobile Phase A:Mobile Phase B for 0.5 minutes.
4

5 MS method: MRM at 342.1/203.1 (1-OH-midazolam) and 346.1/203.1 (α -hydroxymidazolam- d_4) us-
6
7 ing TurboIon spray under positive ion conditions. Nebulizer gas: 12 psi; Curtain gas: 8 psi; IonSpray
8
9 voltage: 2500 V; Source temperature: 500 °C; Declustering potential: 26 V; Focusing potential: 100 V;
10
11 Entrance potential: 4 V; Dwell time 200 ms. Area ratios (metabolite area / stable label metabolite inter-
12
13 nal standard) were determined for 30 minute inactivation incubations with inhibitor and compared with
14
15 incubations containing solvent only (vehicle control). Percent inhibition was calculated by $100 - (\text{area}$
16
17 $\text{ratio } 30 \text{ minute inactivation} / \text{area ratio } 0 \text{ minute inactivation} \times 100)$.
18
19
20
21

22 **Solubility Assays.** The test compound (2 mg) was treated with the solubility medium (FasSIF or 0.1N
23
24 aqueous HCl, 1.0 mL) and agitated at 25 rpm at room temperature for 24 h. The resulting slurry was
25
26 centrifuged at 14000 rpm (16873 rcf) with a 0.45 μm centrifugal filter for 2 min. The pH of the filtrate
27
28 was measured, and the concentration of dissolved drug was measured by HPLC analysis.
29
30

31 ***In vivo studies.***

32
33
34 The pharmacokinetic and plasma exposure animal experiments are protocol driven studies. All proce-
35
36 dures in the protocols are in compliance with the U.S. Department of Agriculture (USDA) Animal Wel-
37
38 fare Act (9CFR Parts 1, 2, and 3); the Guide for the Care and Use of Laboratory Animals from the Insti-
39
40 tute of Laboratory Animal Resources, National Academy Press, Washington, D.C., 1996; and the Na-
41
42 tional Institutes of Health, Office of Laboratory Animal Welfare.
43
44

45
46 **Pharmacokinetic:** Male Beagle dogs (9.2 to 12.7 kg, $N = 3/\text{dose group}$) were administered test com-
47
48 pounds as an intravenous (bolus) solution and oral (gavage) suspension. Blood (approximately 1
49
50 mL/timepoint) was collected from the jugular vein at 0.08 (IV only), 0.25, 0.5, 1, 2, 4, 8, 12, and 24
51
52 hours post dose into tubes containing EDTA anti-coagulant. Blood samples were centrifuged (3000
53
54 RPM for 10 minutes at 4°C), plasma was removed and stored at approximately -60 °C until analyzed.
55
56
57
58
59
60

1 Plasma concentrations of test compounds were determined using an LC/MS-MS bioanalytical method
2
3 (test compound concentration curve range = 1 to 5000 ng/mL).
4

5 **Plasma exposure (free base vs phosphate salt comparison):** Male Beagle dogs (9.1 to 12.7 kg, $N =$
6
7 6/dose group) were administered test compounds as oral (gavage) suspensions. The phosphate salt dose
8 was corrected to give the dose as free base equivalents. Blood (approximately 1 mL/timepoint) was col-
9 lected from the jugular vein at 0.25, 0.5, 1, 2, 4, 8, 12, 24 and 48 hours post dose into tubes containing
10 EDTA anti-coagulant. Blood samples were centrifuged (3000 RPM for 10 minutes at 4°C), plasma was
11 removed and stored at approximately -20 °C until analyzed. Plasma concentrations of test compounds
12 were determined using an LC/MS-MS bioanalytical method (test compound, as free base, concentration
13 curve range = 1 to 20000 ng/mL).
14
15
16
17
18
19
20
21
22
23

24 ASSOCIATED CONTENT

25 Supporting Information

26
27
28 Procedures for the preparation of **5–7**, **9–10**, **20–25** and **27–30**, crystallization and structural determina-
29 tion, A549 assay PGI₂ data, HWB assay TXB₂ and PGF_{2α} data, and CEREP panel results. This material
30 is available free of charge via the Internet at <http://pubs.acs.org>.
31
32
33
34
35
36
37

38 Accession codes

39
40 Coordinates and structure factors are available from the Protein Data Bank with accession codes 5BQG,
41 5BQH, and 5BQI for *m*PGES-1/4, *m*PGES-1/5, and *m*PGES-1/8 binary complexes, respectively.
42
43
44
45

46 AUTHOR INFORMATION

47 Corresponding Author

48
49 * (M.A.S.) E-mail: schifflerma@lilly.com; Tel: +1-317-433-4994.
50
51
52
53

54 Present Addresses

55
56
57 † Retired.
58
59
60

‡ Department of Biotechnology and Food Science, Mongolia International University, 13th Khoroo, Bayanzürkh Dүүreg, Ulaanbaatar, Mongolia.

§ Novartis Institutes for Biomedical Research, Cambridge, MA, USA.

Author Contributions

All authors have given approval to the final version of the manuscript.

Notes

The authors declare no competing financial interest.

ACKNOWLEDGMENT

The authors thank Jeffrey Nissen for valuable synthetic contributions, Ashley Sloan and Robin Kizer for obtaining data in the enzyme assay, and Dan Mudra and Mike Mohutsky for helping prepare the Supporting Information.

The authors gratefully acknowledge dog live phase support from Covance and bioanalytical support from Advion (now a part of Quintiles).

This research used resources of the Advanced Photon Source, a U.S. Department of Energy (DOE) Office of Science User Facility operated for the DOE Office of Science by Argonne National Laboratory under Contract No. DE-AC02-06CH11357.

Use of the Lilly Research Laboratories Collaborative Access Team (LRL-CAT) beamline at Sector 31 of the Advanced Photon Source was provided by Eli Lilly Company, which operates the facility.

ABBREVIATIONS

A₄₁₂, absorbance at $\lambda = 412$ nm; Arg, arginine; BOP, (Benzotriazol-1-yloxy)tris (dimethylamino)phosphonium hexafluorophosphate, CL, clearance; CL_{iv}, clearance after iv dosing; cPGES; cytosolic prostaglandin E synthase; DHPC, 1,2-diheptanoyl-*sn*-glycero-3-phosphocholine; DIEA, diisopro-

1 pylethylamine; DWB, dog whole blood; EIA, enzyme immune assay; FasSIF, fasted state simu-
2 lated
3 intestinal fluid; Gln, glutamine; GTT, glutathione (reduced form); HEPES, (4-(2-hydroxyethyl)-1-
4 piperazineethanesulfonic acid; His, histidine; HLB, hydrophilic-lipophilic balance; HWB, human whole
5 blood; Ile, isoleucine; inh, inhibition; *m*PGES, microsomal prostaglandin E synthase; MRM, multiple
6 reaction monitoring; NMM, 4-methylmorpholine; NT, not tested; PGD, prostaglandin D; PGE, prosta-
7 glandin E; PGF, prostaglandin F; PGG, prostaglandin G; PGH, prostaglandin H; PGI, prostaglandin I;
8 rcf, relative centrifugal force; RH, relative humidity; rhIL-1 β , recombinant human interleukin 1 β ; rpm,
9 rotations per minute; SD, standard deviation; Ser, serine; T3P, propylphosphonic anhydride; TBTU, 2-
10 (1H-Benzotriazole-1-yl)-1,1,3,3-Tetramethyluronium tetrafluoroborate; TDI, time-dependent CYP inhi-
11 bition; TXA, thromboxane A; TXB, thromboxane B; $V_{d,ss}$, steady-state volume of distribution; VWD,
12 variable wavelength detector.
13
14
15
16
17
18
19
20
21
22
23
24
25
26

27 REFERENCES

- 28
29
30 (1) Stone, E. An Account of the Success of the Bark of the Willow in the Cure of Agues. *Philos.*
31 *Trans.* **1763**, *53*, 195–200.
32
33
34 (2) Norn, S., Permin, H., Kruse, P. R. & Kruse, E. From willow bark to acetylsalicylic acid. *Dansk*
35 *Medicinhistorisk Årbog* **2009**, *37*, 79–98.
36
37
38 (3) Piria, R. Untersuchungen über das Salicin und die daraus entstehenden Producte. *Ann. Pharm.*
39 **1839**, *30*, 151–185.
40
41
42 (4) Vane, J. R. Inhibition of Prostaglandin Synthesis as a Mechanism of Action for Aspirin-like
43 Drugs. *Nature New Biology* **1971**, *231*, 232–235.
44
45
46 (5) Smith, J. B.; Willis, A. L. Aspirin Selectively Inhibits Prostaglandin Production in Human Plate-
47 lets. *Nature New Biology* **1971**, *231*, 235–237.
48
49
50 (6) Ferreira, S. H., Moncada, S.; Vane, J. R. Indomethacin and Aspirin abolish Prostaglandin Release
51 from the Spleen. *Nature New Biology* **1971**, *231*, 237–240.
52
53
54
55
56
57
58
59
60

- 1
2
3
4
5
6
7
8
9
10
11
12
13
14
15
16
17
18
19
20
21
22
23
24
25
26
27
28
29
30
31
32
33
34
35
36
37
38
39
40
41
42
43
44
45
46
47
48
49
50
51
52
53
54
55
56
57
58
59
60
- (7) Burch, J. W.; Stanford, N.; Majerus, P. W. Inhibition of platelet prostaglandin synthetase by oral aspirin. *J. Clin. Invest.* **1978**, *61*, 314–319.
- (8) Laneuville, O., Breuer, D. K., DeWitt, D. L. Differential inhibition of human prostaglandin endoperoxide H synthases-1 and -2 by nonsteroidal anti-inflammatory drugs. *J. Pharmacol Exp. Ther.* **1994**, *271*, 927–934.
- (9) Seibert, K.; Masferrer, J. L. Role of inducible cyclooxygenase (COX-2) in inflammation. *Receptor* **1994**, *4*, 17–23.
- (10) Hawkey, C. J. Cox-2 Inhibitors. *The Lancet* **1999**, *353*, 307–314.
- (11) Chen, Y.-F.; Jobanputra, P.; Barton, P.; Bryan, S.; Fry-Smith, A.; Harris, G.; Taylor, R. S. Cyclooxygenase-2 selective non-steroidal anti-inflammatory drugs (etodolac, meloxicam, celecoxib, rofecoxib, etoricoxib, valdecoxib and lumiracoxib) for osteoarthritis and rheumatoid arthritis: a systematic review and economic evaluation. *Health Technology Assessment* **2008**, *12*, 1–278.
- (12) Moncada, S.; Vane, J. R. Interrelationships between prostacyclin and thromboxane A₂. *Ciba Found. Symp.* **1980**, *78*, 165–183.
- (13) Sun, S. X.; Lee, K. Y.; Bertram, C. T.; Goldstein, J. L. Withdrawal of COX-2 selective inhibitors rofecoxib and valdecoxib: impact on NSAID and gastroprotective drug prescribing and utilization. *Curr. Med. Res. Opin.* **2007**, *23*, 1859–1866.
- (14) Samuelsson, B.; Morgenstern, R.; Jakobsson P. J. Membrane prostaglandin E synthase-1: a novel therapeutic target. *Pharmacol. Rev.* **2007**, *59*, 207–224.
- (15) Jakobsson, P.-J.; Thorén, S.; Morgenstern, R.; Samuelsson, B. Identification of human prostaglandin E synthase: A microsomal, glutathione-dependent, inducible enzyme, constituting a potential novel drug target. *Proc. Natl. Acad. Sci. USA* **1999**, *96*, 7220–7225.
- (16) Chang, H.-H.; Meuillet, E. J. Identification and development of mPGES-1 inhibitors: where we are at? *Future Med. Chem.* **2011**, *3*, 1909-1934.

1 (17) See Takusagawa, F. Microsomal prostaglandin E synthase type 2 (mPGES2) is a glutathione-
2 dependent heme protein, and dithiothreitol dissociates the bound heme to produce active prostaglandin
3 E2 synthase in vitro. *J. Biol. Chem.* **2013**, *288*, 10166–10175 and references therein.

4
5
6
7 (18) Bahia, M. S.; Katare, Y. K.; Silakari, O.; Vyas, B.; Silakari, P. Inhibitors of Microsomal Prosta-
8 glandin E2 Synthase-1 Enzyme as Emerging Anti-Inflammatory Candidates. *Med. Res. Rev.* **2014**, *34*,
9 825–855.

10
11
12
13 (19) Abdul-Malik, H. M.; Akasaka, H.; Ruan, K. H. Current Advances of Microsomal Prostaglandin E
14 Synthase-1 as a Target in Inflammation and Cancer. *Am. J. Integrative Med.*, **2013**, *3*, 2–11.

15
16
17 (20) Xu, D.; Rowland, S. E.; Clark, P.; Giroux, A.; Côté, B.; Guiral, S.; Salem, M.; Ducharme, Y.;
18 Friesen, R. W.; Méthot, N.; Mancini, J.; Audoly, L.; Riendeau, D. MF63 [2-(6-chloro-1H-phenanthro
19 [9,10-d] imidazol-2-yl)-isophthalonitrile], a selective microsomal prostaglandin E synthase-1 inhibitor,
20 relieves pyresis and pain in preclinical models of inflammation. *J. Pharmacol. Exp. Ther.*, **2008**, *326*,
21 754–763.

22
23
24 (21) Riendeau, D.; Aspiotis, R.; Ethier, D.; Gareau, Y.; Grimm, E. L.; Guay, J.; Guiral, S.; Juteau, H.;
25 Mancini, J. A.; Méthot, N.; Rubin, J.; Friesen, R. W. Inhibitors of the inducible microsomal prostaglan-
26 din E2 synthase (mPGES-1) derived from MK-886. *Bioorg. Med. Chem. Lett.* **2005**, *15*, 3352–3355.

27
28
29 (22) Mbalaviele, G.; Pauley, A. M.; Shaffer, A. F.; Zweifel, B. S.; Mathialagan, S.; Mnich, S. J.;
30 Nemirovskiy, O. V.; Carter, J.; Gierse, J. K.; Wang, J. L.; Vazquez, M. L.; Moore, W. M.; Masferrer, J.
31 L. Distinction of microsomal prostaglandin E synthase-1 (mPGES-1) inhibition from cyclooxygenase-2
32 inhibition in cells using a novel, selective mPGES-1 inhibitor. *Biochem. Pharmacol.* **2010**, *79*, 1445–
33 1454.

34
35
36 (23) Arhancet, G. B.; Walker, D. P.; Metz, S.; Fobian, Y. M.; Heasley, S. E.; Carter, J. S.; Springer, J.
37 R.; Jones, D. E.; Hayes, M. J.; Shaffer, A. F.; Jerome, G. M.; Baratta, M. T.; Zweifel, B.; Moore, W. M.;
38 Masferrer, J. L.; Vazquez, M. L. Discovery and SAR of PF-4693627, a potent, selective and orally bio-
39
40
41
42
43
44
45
46
47
48
49
50
51
52
53
54
55
56
57
58
59
60

1 available mPGES-1 inhibitor for the potential treatment of inflammation. *Bioorg. Med. Chem. Lett.*

2
3 **2013**, *23*, 1114–1119.

4
5 (24) To our knowledge, the structure of GRC27864 has not been disclosed. See: GRC 27864 First in
6
7 Man, Single Ascending Dose Study in Healthy Volunteers.

8
9 <http://clinicaltrials.gov/ct2/show/NCT02179645>.

10
11 (25) See Supporting Information for details.

12
13 (26) Huntjens, D. R. H.; Danhof, M.; Della Pasqua, O. E. Pharmacokinetic–pharmacodynamic corre-
14
15 lations and biomarkers in the development of COX-2 inhibitors. *Rheumatology* **2005**, *44*, 846–859.

16
17 (27) Due to the short half-life of TXA₂, TXB₂ is frequently used as a marker for TXA₂ production.
18
19 See: Kyrle, P. A.; Eichler, H. G.; Jäger, U.; Lechner, K. Inhibition of prostacyclin and thromboxane A₂
20
21 generation by low-dose aspirin at the site of plug formation in man in vivo. *Circulation* **1987**, *75*, 1025–
22
23 1029.

24
25 (28) Tacconelli, S.; Capone, M. L.; Sciulli, M. G.; Ricciotti, E.; Patrignani, P. The Biochemical Se-
26
27 lectivity of Novel COX-2 Inhibitors in Whole Blood Assays of COX-isozyme Activity. *Curr. Med. Res.*
28
29 *Opin.* **2002**, *18*, 503–511.

30
31 (29) In our hands, the IC₅₀ of celecoxib for PGE₂ reduction in LPS-stimulated HWB was 425 nM ×/÷
32
33 2.00 (*n* = 372). See Supporting Information.

34
35 (30) Paulson, S. K.; Vaughn, M. B.; Jessen, S. M.; Lawal, Y.; Gresk, C. J.; Yan, B.; Maziasz, T. J.;
36
37 Cook, C. S.; Karim, A. Pharmacokinetics of Celecoxib after Oral Administration in Dogs and Humans:
38
39 Effect of Food and Site of Absorption. *J. Pharmacol. Exp. Ther.* **2001**, *297*, 638–648.

40
41 (31) All IC₅₀ and IC₈₀ values are reported as geometric means times or divided by geometric standard
42
43 deviations.

44
45 (32) Luz, J. G.; Antonysamy, S.; Kuklish, S. L.; Condon, B.; Lee, M.; Allison, D.; Yu, X.-P.; Backer,
46
47 R.; Zhang, A.; Russell, M.; Chang, S. S.; Harvey, A.; Sloan, A. V.; Fisher, M. J. Crystal Structures of
48
49
50
51
52
53
54
55
56
57
58
59
60

mPGES-1 Inhibitor Complexes Form a Basis for the Rational Design of Potent Analgesic and Anti-inflammatory Therapeutics. *J. Med. Chem.* **2015**, *58*, 4727–4737.

(33) For additional results from the A549 and HWB assays, see Supporting Information.

(34) COX inhibition was determined using assays essentially as described in Reference 30.

(35) Riley, R. J.; Grime, K.; Weaver, R. Time-dependent CYP inhibition. *Expert Opin. Drug. Metab. Toxicol.* **2007**, *3*, 51–66.

(36) De Bruin, M. L.; Pettersson, M.; Meyboom, R. H. B.; Hoes, A. W.; Leufkens, H. G. M. Anti-HERG activity and the risk of drug-induced arrhythmias and sudden death. *Eur. Heart J.* **2005**, *26*, 590–597.

(37) See Supporting Information for further *in vitro* characterization of **8** and **26**.

(38) Leclerc, P.; Pawelzik, S.-C.; Idborg, H.; Spahiu, L.; Larsson, C.; Stenberg, P.; Korotkova, M.; Jakobsson, P.-J. Characterization of a new mPGES-1 inhibitor in rat models of inflammation. *Prostaglandins and Other Lipid Mediators* **2013**, *102–103*, 1–12.

(39) Due to the inability of **8** and **26** to inhibit rat or mouse mPGES-1, *in vivo* efficacy studies in those species were untenable. However, efficacy studies were performed in guinea pigs and will be reported in due course. See: Chandrasekhar, S.; Harvey, A. K.; Yu, X.-P.; Chambers, M. G.; Oskins, J. L.; Lin, C.; Seng, T. W.; Thibodeaux, S. J.; Norman, B. H.; Hughes, N. E.; Schiffler, M. A.; Fisher, M. J. *Manuscript in preparation*.

(40) Brouwers, J.; Brewster, M. E.; Augustijns, P. Supersaturating drug delivery systems: The answer to solubility-limited oral bioavailability? *J. Pharm. Sci.* **2009**, *98*, 2549–2572.

(41) Takano, R.; Takata, N.; Saito, R.; Furumoto, K.; Higo, S.; Hayashi, Y.; Machida, M.; Aso, Y.; Yamashita, S. Quantitative Analysis of the Effect of Supersaturation on *in Vivo* Drug Absorption. *Mol. Pharmaceutics* **2010**, *7*, 1431–1440.

(42) Performed per the procedure described in: Bhattachar, S.; Perkins, E. J.; Tan, J. S.; Burns, L. J. Effect of gastric pH on the pharmacokinetics of a bcs class II compound in dogs: Utilization of an artifi-

1 cial stomach and duodenum dissolution model and gastroplus,TM simulations to predict absorption. *J.*

2 *Pharm. Sci.* **2011**, *100*, 4756–4765.

3 (43) Bartroli, J.; Turmo, E.; Alguero, M.; Boncompte, E.; Vericat, M. L.; Garcia-Rafanell, J.; Forn, J.

4 Synthesis and Antifungal Activity of New Azole Derivatives Containing an *N*-Acylmorpholine Ring. *J.*

5 *Med. Chem.* **1995**, *38*, 3918–3932.

6 (44) Fajgelj, S.; Stanovnik, B.; Tišler, M. Transformations of *N*-Heteroarylformamidines. A Novel

7 Synthesis of Imidazo/2,1-b/thiazole and Imidazo/2,1-b//1,3,4/thiadiazole Derivatives. *Heterocycles*

8 **1986**, *24*, 379–386.

9 (45) Desirant, Y. Ethyl difluoroacetylacetate. *Bull. Soc. Chim. Belg.* **1930**, *39*, 143–156.

10 (46) Vorbrueggen, H. Esterification of Carboxylic Acids and Etherification of Phenols with Amide

11 Acetals. *Synlett* **2008**, 1603–1617.

12 (47) Leeson, P. D.; Springthorpe, B. The influence of drug-like concepts on decision-making in me-

13 dicinal chemistry. *Nature Review Drug Discovery* **2007**, *6*, 881–890.

14 (48) Zhang, L.; Peng, X.-M.; Damu, G. L. V.; Geng, R.-X.; Zhou, C.-H. Comprehensive Review in

15 Current Developments of Imidazole-Based Medicinal Chemistry. *Med. Res. Rev.* **2014**, *34*, 340–437.

16 (49) Ritchie, T. J.; Macdonald, S. J. F.; Young, R. J.; Pickett, S. D. The impact of aromatic ring count

17 on compound developability: further insights by examining carbo- and hetero-aromatic and -aliphatic

18 ring types. *Drug Discovery Today* **2011**, *16*, 164–171.

19 (50) Einhorn, A.; Bischkopff, E.; Szelinski, B.; Schupp, G.; Spröngerts, E.; Ladisch, C.; Mauermay-

20 er, T. Über die *N*-Methylolverbindungen der Säureamide [Erste Abhandlung]. *Liebigs Ann. Chem.*

21 **1905**, *343*, 207–305.

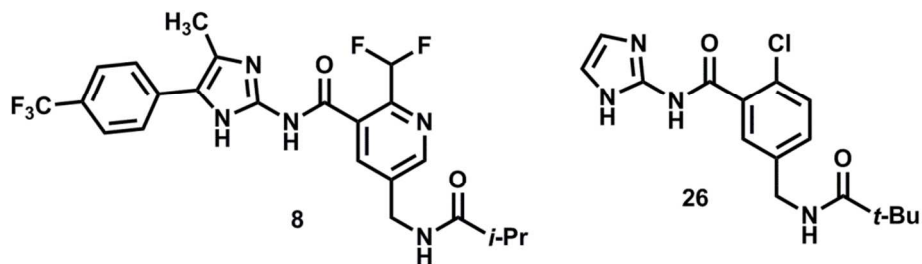
22 (51) Tscherniac, J. Verfahren zur Darstellung von Benzylphthalimiden. German Patent 134,979, Jun 2,

23 1901.

24 (52) As of September 2015, available from AstaTech, Inc. (catalog # CL9222) and Zylexa Pharma

25 (catalog # ZP-DC002387), among other suppliers.

Insert Table of Contents artwork here

1
2
3
4
5
6
7
8
9
10
11
12
13
14
15
16
17
18
19
20
21
22
23
24
25
26
27
28
29
30
31
32
33
34
35
36
37
38
39
40
41
42
43
44
45
46
47
48
49
50
51
52
53
54
55
56
57
58
59
60